Effect of momentum transfer on the acoustic boundary condition of perforated liner walls with grazing flow

Anita Schulz, Dirk Ronneberger

EFFECT OF MOMENTUM TRANSFER ON THE ACOUSTIC BOUNDARY CONDITION OF PERFORATED LINER WALLS WITH GRAZING FLOW

Anita Schulz[1] **Dirk Ronneberger**[2]

[1] Technical University Berlin, 10623 Berlin, Germany
[2] retired, formerly Drittes Physikalisches Institut, 37077 Göttingen, Germany
anita.schulz@dlr.de

ABSTRACT

The interaction between sound and flow at sound-absorbing walls, especially the effect of the unsteady momentum transfer between flow and wall is the subject of the current project. The physical mechanisms of the sound-flow interaction are analyzed for two generic wall types. While the mechanisms at the homogeneously permeable wall are largely understood, the aim is now to transfer these findings to walls with separated openings.

1 INTRODUCTION

When designing and predicting the sound damping performance of acoustic liners, it is crucial that the lined wall is described by a correct acoustical boundary condition. Usually, the effect of a lined wall on the sound field is described by the wall admittance $Y_\mathrm{w} = -\widetilde{v}_\mathrm{w}/\widetilde{p}_\mathrm{w}$, i.e. the ratio of the wall-normal particle velocity directing into the wall and the sound pressure at the wall. This is correct if the fluid is at rest, except for a small correction if the viscous effects are taken into account. It is still correct if a grazing mean flow is superimposed, as in many technical applications like aero engines or exhaust ducts, as long as the wall can be regarded as flexible and impermeable (like a membrane).

However, in reality liners mostly consist of perforated walls (see Fig. 1), i.e. the wall is rigid and permeable.

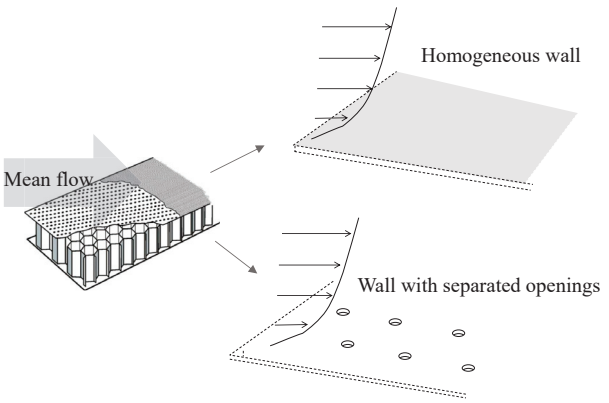

Figure 1. Two wall models for a perforated liner.

Then, the acoustic boundary condition is not only quantitatively but qualitatively changed, because the acoustic flow through the perforations leads to an alternating exchange of streamwise momentum between the mean flow and the wall. This momentum transfer acts like an acoustically streamwise force that the wall exerts on the adjacent fluid, and (actio=reactio) vice versa, the flow exerts on the wall. This force strongly increases with the mean flow velocity and exceeds the value without flow by orders of magnitude.

If at all, the shear stress effects with superimposed mean flow have so far been modeled by the simplifying assumption of a homogeneous wall [1–5] which is not in agreement with realistic liner surfaces where the permeable and the rigid areas are clearly separated from each other. In a previous approach [6, 7] we have described the streamwise force averaged over the wall area, despite of its local mechanisms, as a global acoustic wall shear stress $\widetilde{\tau}_\mathrm{w}$. We have introduced its proportionality to the wall-normal particle velocity as momentum transfer impedance

$$Z_T = -\frac{\widetilde{\tau}_\mathrm{w}}{\widetilde{v}_\mathrm{w}} \tag{1}$$

in accordance with the wall impedance $Z_\mathrm{w} = -\widetilde{p}_\mathrm{w}/\widetilde{v}_\mathrm{w}$. Later, Aurégan [8] has proposed a similar parameter, the 'equivalent friction coefficient' where $\widetilde{\tau}_\mathrm{w}$ is normalized to $\widetilde{p}_\mathrm{w}$.

In [7] we have shown measurements of Z_T at a SDOF resonator liner, based on the assumption that it is an independent and locally reacting wall parameter and forms, together with Z_w, a complete boundary condition. This working hypothesis is questioned in the present work.

In the study to be presented here, we take up from this and examine the physical mechanisms which govern the dynamics of the shearing viscous flow above realistic liner surfaces. To this end, two types of walls have been distinguished which behave differently with respect to origin and propagation of the wall shear stress: a) the homogeneously permeable wall and b) the wall with macroscopic separated openings (see Fig. 1), where the permeable and the rigid no-slip areas are clearly separated from each other and the respective flow acoustic effects need to be modeled separately before homogenization. By investigation of the two types we seek to understand and model the properties of a realistic liner in a way that builds up step by step.

We start with the investigation of a homogeneous wall in Section 3 and 4, before we focus on the differences between the acoustic response of homogenous and inhomogeneous walls in Section 5. This latter investigation is still in progress; so only first results will be presented here. In Section 2 the definition of homogenous and inhomogeneous will be substantiated.

2 DIFFERENTIATION OF WALL TYPES

2.1 Homogeneously permeable wall

The flow near the wall, subject to unsteady boundary conditions – e.g. due to sound superposition – depends, among others, on two essential length scales, namely the length unit $\delta_\nu := \nu/u_\tau$ of the wall mean flow and the acoustic boundary layer thickness $\delta_a = \sqrt{2\nu/\omega}$, with the angular frequency ω, the kinematic viscosity ν and the friction velocity u_τ. In the case of the homogeneously permeable, but rigid (inflexible) wall it is assumed that the size L_{op} of the openings and their spacing L_{sp} are small compared to these two length scales. In practically all technical realizations of liners, however, $L_{op}, L_{\text{sp}} \gg \delta_\nu, \delta_a$. Yet, the model of the homogeneous wall has been used in most previous studies of the shear stress effects, probably due to its beneficial features: 1) $Y_{\text{w}}, Z_{\text{w}}$ are constants and $\widetilde{v}_{\text{w}}$ and $\widetilde{\tau}_{\text{w}}$ are continuous and 2) the no slip condition holds everywhere, i.e., $\overline{u} \equiv 0$ and $\widetilde{u} \equiv 0$ uniformly applies at the wall ($y = 0$) for the x-component of the flow velocity.
The latter can be seen as cause for the shear stress: The convective streamwise velocity at the wall $\widetilde{u}_{\text{slip}} = -(\mathrm{d}\overline{u}/\,\mathrm{d}y)_{\text{w}}\widetilde{\xi}_{\text{w}}$ that would be observed at the wall if the no slip condition would be 'switched off', must be stopped by means of a wall-normal gradient of the shear stress in order to fulfill the no slip condition. This unsteady shear stress diffuses in form of a shear stress wave into the adjacent medium.

2.2 Wall with macroscopic separated openings

As mentioned before, the openings are macroscopic and separated, $L_{\text{op}}, L_{\text{sp}} \gg \delta_\nu, \delta_a$, at a real liner. So we have to differentiate between the dynamics of the flow at the open and at the rigid areas of the wall before a homogenization can be applied.
The main effects of the sound-flow interaction take place in the surrounding of the openings. So we start with a qualitative description of the grazing mean flow over a single slit and a sketch of the associated unsteady forces that locally act on the wall in Fig. 2. In front of the slit ($x < 0$), the velocity profile is governed by the wall shear stress and the transport of axial momentum towards the wall due to viscosity and eventually turbulent convection. Behind the leading edge ($x > 0$), however, the wall shear stress has suddenly disappeared while the momentum transport is still active. So the fluid elements at $y \approx 0$ are strongly accelerated and the streamlines are bent towards the developing shear layer above the slit. Nevertheless, because of zero flux through the slit, the wall streamline starting at

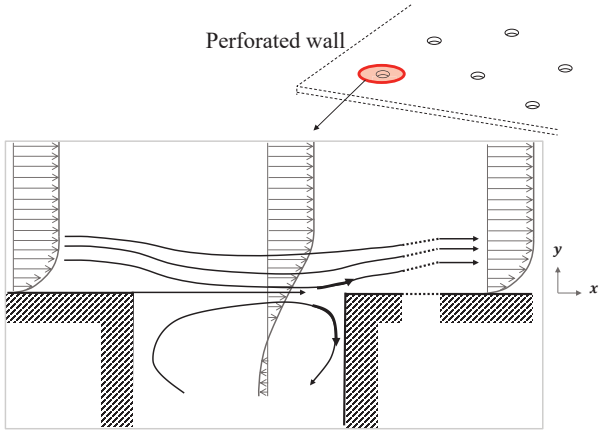

Figure 2. Side view of a grazing mean flow across a slit (no flow through the slit).

the leading edge reaches the rear of the slit exactly at the trailing edge at a velocity $\bar{u}_{\text{te}}$ which is in the order of the flow velocity $\bar{u}_\infty$ outside the boundary layer. Two effects are expected to take place at the trailing edge: a) the accelerated fluid elements for $y < 0$ need to be stopped by the rear side wall, so a region of stagnation pressure forms; b) the flow behind the trailing edge at $y > 0$ is subject to the no-slip condition, where the wall shear stress increases due to the deceleration of fluid elements that hit the trailing edge.
If we now switch on an acoustic flow through the opening $\widetilde{v}_{\text{op}}$ (caused e.g. by the pressure and the admittance of the opening) the flow profile across the slit will alternatingly be sucked in and blew out, as shown in Fig. 3. Hence, not

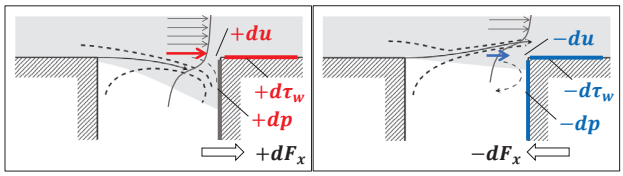

Figure 3. Streamlines above the opening during the in- and the outflow phase of the acoustic flow through the slit.

only the streamwise velocity at the trailing edge ($y = 0$) gets an acoustic component $\widetilde{u}_{\text{te}}$, but also the stagnation pressure and the wall shear stress at the trailing region of the opening are acoustically modulated. Both effects act like a streamwise acoustic force between the mean flow and the wall and it is to be investigated whether and how they contribute to the effective boundary condition of the wall.

3 GOVERNING EQUATIONS

We start from the general linearized equations for the conservation of momentum

$$\frac{\partial \widetilde{\mathbf{u}}}{\partial t} + (\widetilde{\mathbf{u}} \cdot \nabla)\overline{\mathbf{u}} + (\overline{\mathbf{u}} \cdot \nabla)\widetilde{\mathbf{u}} + \frac{\widetilde{\rho}}{\overline{\rho}}(\overline{\mathbf{u}} \cdot \nabla)\overline{\mathbf{u}} = \frac{1}{\overline{\rho}}\nabla\widetilde{p} + \frac{1}{\overline{\rho}}\nabla \cdot \widetilde{\boldsymbol{\tau}} - \nabla \cdot \widetilde{\mathbf{r}} \quad (2)$$

and of mass

$$\frac{\partial \widetilde{\rho}}{\partial t} + (\overline{\mathbf{u}} \cdot \nabla)\widetilde{\rho} + \overline{\rho}\nabla \cdot \widetilde{\mathbf{u}} = 0 \quad (3)$$

and we apply the following assumptions:

- We consider a plane 2d flow with velocity components $\boldsymbol{u}(x, y) = [u, v]^T$ above a straight duct wall positioned at $y = 0$. See also the coordinate system in Fig. 4. The mean flow $\overline{u}(y)$ is wall-parallel and homogeneous in x-direction ($\partial\overline{u}/\partial x = 0$).
- The mean flow is supposed to be low-Mach-number and incompressible, i.e., $(\overline{\rho}, \overline{p}) = (\rho_0, p_0)$ are constants and $\nabla \cdot \overline{\mathbf{u}} = 0$.
- The acoustic quantities $\widetilde{\mathbf{u}}, \widetilde{p}, \widetilde{\rho}, \widetilde{\boldsymbol{\tau}}$ are proportional to $\exp(i\omega t - ik_x x)$ with axial wavenumber k_x and angular frequency ω.
- We completely disregard thermal effects like heat conduction and production of heat (due to shear stress times shear rate), i.e., we adopt the isentropic relation between pressure and density $\widetilde{\rho} = \widetilde{p}/c^2$ with the sound speed $c_0 = \sqrt{\gamma p_0/\rho_0}$ and the adiabatic exponent γ. The mean temperature and the speed of sound c_0 are constants (no spatial variation).
- The turbulence is neglected, i.e. the turbulent stress tensor $\widetilde{\mathbf{r}}$ in Eqn. 2 is zero. The dynamic viscosity μ_0 is presumed to be a constant.
- We neglect the normal stresses of the acoustic part of the viscous stress tensor $\widetilde{\boldsymbol{\tau}} = \left[\begin{smallmatrix} \widetilde{\tau}_{xx} & \widetilde{\tau}_{xy} \\ \widetilde{\tau}_{xy} & \widetilde{\tau}_{yy} \end{smallmatrix}\right]$, since they are small compared to the shear stresses $\widetilde{\tau}_{xy}$. Only the shear stress $\widetilde{\tau}_{xy} =: \widetilde{\tau}$ is retained in Eqn. 2.
- We avoid critical layers, e.g. the phase velocity of the sound wave $\omega/k_x \neq \overline{u}$ for all wall distances y.

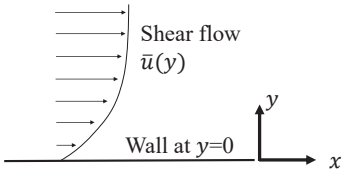

Figure 4. Used coordinate system.

The customized momentum equations in x and in y direction then reads

$$i(\omega - k_x\overline{u})\widetilde{u} + \widetilde{v}\frac{d\overline{u}}{dy} = \frac{ik_x}{\rho_0}\widetilde{p} + \frac{1}{\rho_0}\frac{\partial\widetilde{\tau}}{\partial y} \quad (4)$$

$$i(\omega - k_x\overline{u})\widetilde{v} = -\frac{1}{\rho_0}\frac{\partial\widetilde{p}}{\partial y} - \frac{ik_x}{\rho_0}\widetilde{\tau} \quad (5)$$

and the customized continuity equation is:

$$i(\omega - k_x\overline{u})\widetilde{p} + \rho_0 c_0^2\Big(\frac{\partial\widetilde{v}}{\partial y} - ik_x\widetilde{u}\Big) = 0. \quad (6)$$

Eqn. 4-6 together with Eqn. 10 form a system of non-homogeneous first order differential equations with four unknown acoustic variables $\widetilde{u}, \widetilde{v}, \widetilde{\tau}$ and $\widetilde{p}$.
It is now to look for a transformation of Eqn. 4-6 to describe the wavelike diffusion of momentum from the wall into the fluid. We have followed two approaches, one tackles the problem in terms of the shear stress $\widetilde{\tau}$ and the wall-normal particle displacement

$$\widetilde{\xi} = \frac{\widetilde{v}}{i\omega'}, \quad \text{where} \quad \omega' = \omega - k_x\overline{u}(y) \quad (7)$$

is the Doppler shiftet frequency and is a function of the mean flow profile and the streamwise component of the sound wavenumber. The second approach uses a formulation in terms of the components of the particle velocity $\widetilde{u}$ and $\widetilde{v}$.

3.1 System of equations, Form 1 ($\widetilde{\tau}, \widetilde{\xi}$)

The Eqn. 4-6 can be rewritten as

$$\frac{\partial^2\widetilde{\tau}}{\partial y^2} + (k_x^2 - \frac{i\omega'}{\nu})\widetilde{\tau} = i\omega'\rho_0\Big(\frac{\mathrm{d}^2\overline{u}}{\mathrm{d}y^2} - k_x\omega'\Big)\widetilde{\xi} - \frac{i\omega'}{c_0^2}\frac{\mathrm{d}\overline{u}}{\mathrm{d}y}\widetilde{p} \quad (8)$$

$$\frac{\partial\widetilde{\xi}}{\partial y} = -\frac{ik_x}{\rho_0\omega'^2}\frac{\partial\widetilde{\tau}}{\partial y} + \Big(\Big(\frac{k_x c_0}{\omega'}\Big)^2 - 1\Big)\frac{\widetilde{p}}{\rho_0 c_0^2} \quad (9)$$

Eqn. 8 is derived by using

$$\widetilde{\tau} = \mu_0\Big(\frac{\partial\widetilde{u}}{\partial y} + \frac{\partial\widetilde{v}}{\partial x}\Big) \approx \mu_0\frac{\partial\widetilde{u}}{\partial y} \quad (10)$$

with the dynamic viscosity μ_0. The approximation in Eqn. 10 is based on the fact that $\widetilde{u} \gg \widetilde{v}$ and $\kappa \gg k_x$ in our case, $\kappa = \sqrt{i\omega/\nu}$ being a characteristic wavenumber for the shear stress wave. Substituting for $\widetilde{u}$ from Eqn. 4 into Eqn. 10 and using Eqn. 5 to substitute the pressure gradient $\partial\widetilde{p}/\partial y$ yields Eqn. 8. Eqn. 9 is a combination of Eqn. 4 and Eqn. 6.
Eqn. 8 and 9 form a system of two coupled inhomogeneous ODE with non constant coefficients (ω' and $\overline{u}$ are functions of y). Both equations depend (besides the pressure $\widetilde{p}$) on the shear stress $\widetilde{\tau}(y)$ and the displacement $\widetilde{\xi}(y)$. They must therefore be solved simultaneously together with appropriate boundary conditions. The inhomogeneity makes an approximative solution challenging. In Section 4 we show an numerical solution based on a fourth-order compact finite difference scheme.
To derive an approximate solution for the propagation of the shear stress diffusion wave we chose the following, alternative formulation, inspired by the approach of Starobinski [2] and Aurégan et al. [3].

3.2 System of equations, Form 2 ($\widetilde{u}, \widetilde{v}$)

The second formulation is derived from Eqn. 4 where $\widetilde{\tau}$ is replaced by Eqn. 10

$$\frac{\partial^2 \widetilde{u}}{\partial y^2} - \frac{i\omega'}{\nu}\widetilde{u} = \frac{1}{\nu}\frac{\mathrm{d}\overline{u}}{\mathrm{d}y}\widetilde{v} - \frac{i\omega'}{\nu\rho_0}\widetilde{p} \tag{11a}$$

and an alternative version of this equation is obtained by replacing $k_x\widetilde{u}$ by the continuity equation 6:

$$\frac{\partial^2 \widetilde{u}}{\partial y^2} - \frac{i\omega}{\nu}\widetilde{u} = \frac{1}{\nu}\frac{\mathrm{d}\overline{u}}{\mathrm{d}y}\widetilde{v} - \frac{\overline{u}}{\nu}\frac{\partial \widetilde{v}}{\partial y} - \left(\frac{i\omega'\overline{u}}{\nu\rho_0 c_0^2} + \frac{ik_x}{\nu\rho_0}\right)\widetilde{p} \tag{11b}$$

with the kinematic viscosity $\nu = \mu_0/\rho_0$. Eqn. 11 describes the dynamics of the viscous boundary layer in terms of $\widetilde{u}$ and $\widetilde{v}$ instead of $\widetilde{\tau}$ and $\widetilde{\xi}$. In contrast to Eqn. 8 and 11a the coefficients on the left hand side of Eqn. 11b are constants (no y-dependency).

4 SOLUTION FOR THE HOMOGENEOUSLY PERMEABLE WALL

In the following we look for a solution for the propagation of the viscous stress wave, excited at a homogeneous and permeable wall. According to Section 2.1 such kind of wall is characterized (1) by the no slip condition: $\overline{u}_\mathrm{w} = 0$, $\widetilde{u}_\mathrm{w} = 0$ and (2) by the fact that the wall admittance Y_w is independent of x, meaning that the wall-normal displacement at the wall

$$\widetilde{\xi}_\mathrm{w} := \widetilde{\xi}(0) = \frac{\widetilde{v}_\mathrm{w}}{i\omega} = -\frac{Y_\mathrm{w}\widetilde{p}_\mathrm{w}}{i\omega} \tag{12}$$

is a continuous function of x.

The solution for the propagation of the shear stress wave is determined by two scales: By the thickness of the acoustic boundary in the no-flow case, $\delta_a = \sqrt{2\nu/\omega}$, and by the thickness of mean flow wall boundary layer δ_f which scales with $\overline{u}_\infty/(\mathrm{d}\overline{u}/\,\mathrm{d}y)_\mathrm{w} \approx 20\nu/u_\tau$, where $\overline{u}_\infty$ is the mean flow velocity outside of the flow boundary layer ($y \gg \delta_f$). Once the solution for the shear wave is known, we seek to describe the effect of the wall together with the acoustic boundary layer effects by an 'effective boundary condition', seen by the inviscid flow outside the acoustic boundary layer, i.e. where the shear wave has decayed. Since, as we show later, the shear wave is coupled to the mean flow boundary layer, the effective boundary also must be located outside of the flow boundary layer. We call this position y_∞ and the corresponding constant mean flow velocity $\overline{u}_\infty := \overline{u}(y_\infty)$. The effective wall-normal diplacement is a superposition of the displacement $\widetilde{\xi}_w$ due to the compliance of the wall and the 'added displacement' $\widetilde{\xi}_\mathrm{add}$ [2, 3] due to the shear stress wave

$$\widetilde{\xi}_\mathrm{eff} := \widetilde{\xi}(y_\infty) = \widetilde{\xi}_\mathrm{w} + \widetilde{\xi}_\mathrm{add}, \tag{13}$$

where $\widetilde{\xi}_\mathrm{add}$ depends on the solutions for the shear stress wave. The effective wall admittance is

$$Y_\mathrm{eff} = -\frac{\widetilde{v}_\mathrm{w} + \widetilde{v}_\mathrm{add}}{\widetilde{p}_\mathrm{w}} = -\frac{i\omega'_\infty \widetilde{\xi}_\mathrm{eff}}{\widetilde{p}_\mathrm{w}} = Y_\mathrm{w}\frac{\omega'_\infty}{\omega}\left(1 + \frac{\widetilde{\xi}_\mathrm{add}}{\widetilde{\xi}_\mathrm{w}}\right) \tag{14}$$

with $\omega'_\infty = \omega - k_x\overline{u}_\infty$, the Doppler shiftet frequency at y_∞. According to Eqn. 14 $\widetilde{v}_\mathrm{add}$ and $\widetilde{\xi}_\mathrm{add}$ are linked by $\widetilde{v}_\mathrm{add} = i\omega'_\infty\widetilde{\xi}_\mathrm{add} - ik_x\overline{u}_\infty\widetilde{\xi}_\mathrm{w}$.

4.1 Numerical solution

Both formulations for the propagation of the shear stress, the $\widetilde{\tau}, \widetilde{\xi}$-form (Eqn. 8, 9) and the $\widetilde{u}, \widetilde{v}$-form (Eqn. 11) are solved directly by means of a numerical routine. The two solutions are later compared to an approximative solution of Eqn. 11 which is explained in Section 4.2.

4.1.1 Form 1 ($\widetilde{\tau}, \widetilde{\xi}$)

We focus on the shear stress component that is caused by the exchange of momentum between the mean flow and the permeable wall; i.e we will exclude the shear stress caused by the axial pressure gradient, since its contribution to the total shear stress is small or even negligible in most practical cases. So, the pressure terms ($\widetilde{p}$ and $\partial\widetilde{p}/\partial x$) are dropped in Eqn. 8, Eqn. 9 and Eqn. 11.

According to the common boundary layer approximation we assume the pressure $\widetilde{p}$ to be independent of the wall-normal coordinate y in the shear stress layer. Dropping also the terms originating from $\partial\widetilde{p}/\partial y$ in Eqn. 8 (together with the pressure terms) Eqn. 8 and 9 reduce to

$$\frac{\partial^2 \widetilde{\tau}}{\partial y^2} - \frac{i\omega'}{\nu}\widetilde{\tau} = i\omega'\rho_0\frac{\mathrm{d}^2\overline{u}}{\mathrm{d}y^2}\widetilde{\xi} \tag{15}$$

$$\frac{\partial \widetilde{\xi}}{\partial y} = -\frac{ik_x}{\rho_0\omega'^2}\frac{\partial \widetilde{\tau}}{\partial y} \tag{16}$$

Both, Eqn. 15 and 16, are inhomogeneous and have to be simultaneously solved for the shear stress $\widetilde{\tau}(y)$ and the displacement $\widetilde{\xi}(y)$. Note that due to the inhomogeneity of Eqn. 15 the shear stress is not only excited at the wall but everywhere where $\mathrm{d}^2\overline{u}/\,\mathrm{d}y^2$ is noticeable. So the shear stress wave may reach far beyond $y = \delta_a$.

A finite difference scheme of fourth order has been used to solve the Eqn. 15 and 16, together with the two corresponding boundary conditions:

1. The first boundary condition accounts for the general requirement that the shear stress wave has to decay and vanish far away from the wall, $\widetilde{\tau}(y) \to 0$ for $y \to \infty$. Especially, outside of the flow boundary layer ($y \gg \delta_f$), where the mean flow is uniform ($\overline{u} \equiv \overline{u}_\infty$), the right side of Eqn. 15 drops to zero and the Doppler shifted frequency on the left side becomes a constant, $\omega'(y) \equiv \omega'_\infty = \omega - k_x\overline{u}_\infty$. Then, the general solution of Eqn. 15 is composed of two simple exponential functions $\exp(\pm\kappa_\infty y)$ with $\kappa_\infty = \sqrt{i\omega'_\infty/\nu}$, but only the decaying component may survive. Therefore, the boundary condition outside the flow boundary layer is

$$\widetilde{\tau}(y) \sim e^{-\kappa_\infty y} \quad \Rightarrow \quad \frac{\partial \widetilde{\tau}}{\partial y} = -\kappa_\infty\widetilde{\tau} \qquad y \gg \delta_f. \tag{17}$$

2. The second boundary condition is the no-slip condition which requires that the wall-normal gradient of the

shear stress stops the slip velocity $\widetilde{u}_{\text{slip}} = (\mathrm{d}\overline{u}/\,\mathrm{d}y)_{\text{w}}\widetilde{\xi}_{\text{w}}$ with the displacement $\widetilde{\xi}_{\text{w}}$ at the wall

$$\frac{\partial\widetilde{\tau}}{\partial y} = i\omega\rho_0\frac{\mathrm{d}\overline{u}}{\mathrm{d}y}\widetilde{\xi}_{\text{w}} \qquad y = 0 \tag{18}$$

Because of the linearity of the equations $\widetilde{\tau}(y)$ and $\widetilde{\xi}(y)$ will be proportional to $\widetilde{\xi}_{\text{w}}$ which will be set to 1, regardless of the mechanism of its excitation.

In the numerical routine we have used a spatial range of $0 \le y \le y_\infty$ with $y_\infty = \max(10\,\delta_a, 7\,\delta_f)$ to ensure that both boundary layers are fully covered. The distance between the grid points is determined by $\min(\delta_a/N_a, \delta_f/N_f)$, where $N_a = 20, N_f = 20$ have proven to be sufficient.

The effective boundary condition according to Eqn. 13, 14 can be directly evaluated from the numerical solution of $\widetilde{\xi}$ for the point furthest from the wall, $\widetilde{\xi}_{\text{eff}} = \widetilde{\xi}(y_\infty)$.

4.1.2 Form 2 ($\widetilde{u}, \widetilde{v}$)

We have solved Eqn. 11a (with the pressure term set to zero) by the same finite difference as in the previous section. The corresponding boundary conditions are:

1. Outside the flow boundary layer the right hand side of Eqn. 11a vanishs

$$\widetilde{u}(y) \sim e^{-\kappa_\infty y} \quad \Rightarrow \quad \frac{\partial\widetilde{u}}{\partial y} = -\kappa_\infty\widetilde{u}, \qquad y \gg \delta_f. \tag{19a}$$

2. The no slip condition applies at the wall

$$\widetilde{u}_{\text{w}} = 0, \qquad y = 0. \tag{19b}$$

The effective boundary condition according to Eqn. 13, 14 can be directly determined from the numerical solution of $\widetilde{v}$ for the point furthest from the wall, $\widetilde{\xi}_{\text{eff}} = \widetilde{v}(y_\infty)/(i\omega'_\infty)$.

4.2 Approximate solution for form 2 ($\widetilde{u}, \widetilde{v}$)

In order to derive an approximate solution of Eqn. 11 we decompose the wall-normal particle velocity in Eqn. 11b

$$\widetilde{v} = \widetilde{v}_{\text{w}} + \widetilde{v}_\delta, \tag{20}$$

into the constant part $\widetilde{v}_{\text{w}}$ which is the particle velocity at the wall, and a y-dependent residual part $\widetilde{v}_\delta(y)$. Substituting for $\widetilde{v}$ into Eqn. 11b gives

$$\frac{\partial^2\widetilde{u}}{\partial y^2} - \frac{i\omega}{\nu}\widetilde{u} = \frac{1}{\nu}\frac{\mathrm{d}\overline{u}}{\mathrm{d}y}\widetilde{v}_{\text{w}} + \frac{1}{\nu}\frac{\mathrm{d}\overline{u}}{\mathrm{d}y}\widetilde{v}_\delta - \frac{\overline{u}}{\nu}\frac{\partial\widetilde{v}_\delta}{\partial y} \tag{21}$$

Because of the linearity of Eqn. 21 the solution is a superposition of two independent components $\widetilde{u} = \widetilde{u}_1 + \widetilde{u}_2$, each of which satisfies an own equation

$$\frac{\partial^2\widetilde{u}_1}{\partial y^2} - \frac{i\omega}{\nu}\widetilde{u}_1 = \frac{1}{\nu}\frac{\mathrm{d}\overline{u}}{\mathrm{d}y}\widetilde{v}_{\text{w}} \tag{22a}$$

$$\frac{\partial^2\widetilde{u}_2}{\partial y^2} - \frac{i\omega}{\nu}\widetilde{u}_2 = \frac{1}{\nu}\frac{\mathrm{d}\overline{u}}{\mathrm{d}y}\widetilde{v}_\delta - \frac{\overline{u}}{\nu}\frac{\partial\widetilde{v}_\delta}{\partial y}. \tag{22b}$$

So far, we have solved Eqn. 22a for $\widetilde{u}_1$ by the method of variation of constants, where the solution for $\widetilde{u}_2$, which is expected to deliver only a small contribution to the complete solution, is still pending. Thus $\widetilde{u}_1$ is regarded as a first approximation that gives insight into at least part of the important parameter dependencies. We have used the continuity equation 6 (with zero pressure) to determine the added displacement $\widetilde{v}_{\text{add}}$ from $\widetilde{u}_1(y)$

$$\widetilde{v}_{\text{add}} = ik_x\int_0^\infty \widetilde{u}_1\,\mathrm{d}y = \frac{k_x\widetilde{v}_{\text{w}}}{\omega}\left[\int_0^\infty \frac{\mathrm{d}\overline{u}}{\mathrm{d}y}e^{-\kappa_0 y}\,\mathrm{d}y - \overline{u}_\infty\right]. \tag{23}$$

The effective wall-normal displacement normalized to the displacement at the wall is then (see also Eqn. 14)

$$\begin{aligned}\frac{\widetilde{\xi}_{\text{eff}}}{\widetilde{\xi}_{\text{w}}} &= \frac{\omega}{\omega'_\infty}\frac{Y_{\text{eff}}}{Y_{\text{w}}} = \frac{\omega}{\omega'_\infty}\frac{\widetilde{v}_{\text{w}} + \widetilde{v}_{\text{add}}}{\widetilde{v}_{\text{w}}} \\ &= \frac{\omega}{\omega'_\infty}\left[1 + \frac{k_x\overline{u}_\infty}{\omega}\left(\int_0^\infty \frac{\mathrm{d}\overline{u}/\,\mathrm{d}y}{\overline{u}_\infty}e^{-\kappa_0 y}\,\mathrm{d}y - 1\right)\right] \\ &= 1 + \frac{kM_{\text{eff}}}{1 - kM_\infty},\end{aligned} \tag{24a}$$

where $k = c_0k_x/\omega$ is the normalized axial wavenumber, and $M_\infty = \overline{u}_\infty/c_0$ is the Mach number outside the flow boundary layer. The governing parameter of Eqn. 24a is

$$M_{\text{eff}} = \int_0^\infty \frac{\mathrm{d}M}{\mathrm{d}y}e^{-\kappa_0 y}\,\mathrm{d}y, \quad \text{with} \quad \kappa_0 = \sqrt{\frac{i\omega}{\nu}}, \tag{24b}$$

with Mach number $M(y)$. M_{eff} was previously used by Starobinski [2] and Aurégan et al. [3], yet their $\widetilde{\xi}_{\text{eff}}$ differs from Eqn. 24a. From Eqn. 24a it can be concluded that the effective admittance of a homogeneous liner wall becomes non-locally reacting even if the wall admittance itself is locally reacting ($\partial Y_{\text{w}}/\partial k_x = 0$).

4.3 Results and discussion

We have used two analytical flow boundary layer profiles to analyse the results:

$$\text{Exponential:} \quad \overline{u}(y) = \overline{u}_\infty(1 - e^{-ay}) \tag{25a}$$

$$\text{Tanh:} \quad \overline{u}(y) = \overline{u}_\infty\tanh(ay), \tag{25b}$$

where the slope parameter a was adjusted to match the wall shear stress of a turbulent boundary layer. For the friction velocity this yields

$$u_\tau = \sqrt{\overline{\tau}_{\text{w}}/\rho_0} = \sqrt{\nu\,\mathrm{d}\overline{u}/\,\mathrm{d}y} = \sqrt{a\nu\overline{u}_\infty}.$$

Since $u_\tau \approx \overline{u}_\infty/20$, it follows that $a = \overline{u}_\infty/(400\nu)$. Fig. 5 shows the two boundary layer profiles with respect to the wall distance normalized to the flow boundary layer thickness y/δ_f.

4.3.1 Effective displacement

In Fig. 6-10 the results for the effective wall-normal displacement normalized to the displacement at the wall are

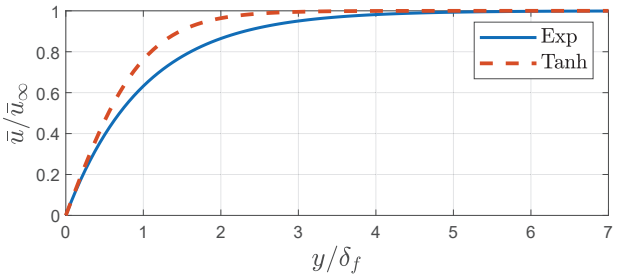

Figure 5. Used flow boundary layer profiles.

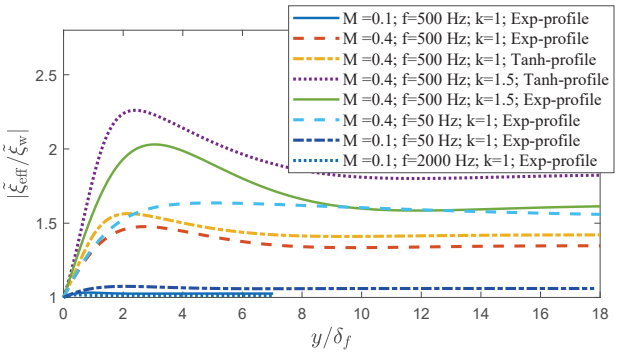

Figure 6. Wall-normal profiles of the effective displacement for various parameter combinations. The y-coordinate is normalized by the mean flow boundary layer thickness (numerical solution).

shown. According to Eqn. 14 this is proportional to the effective admittance of the wall. Only the magnitudes are shown. In Fig. 6 the wall-normal profiles as functions of the normalized wall distance are depicted for different combinations of Mach number $M = \overline{u}_\infty/c_0$, normalized wavenumber $k = c_0 k_x/\omega$, sound frequency, and mean flow profile. All parameters clearly effect the magnitude and the penetration depth of the shear wave. In Fig. 7-9 the dependency on the normalized streamwise wavenumber k is emphasized [1] and the numerical solution is compared to the approximation based on $\widetilde{u}_1$ (Eqn. 24) as well as to the approximation by other authors [1–3].

It turns out that the effective displacement is to first order of M a linear function of the wavenumber, and the dependency on k_x increases with growing Mach number and decreasing frequency. Interestingly, the approximation by Aurégan et al. [3] is superior to all other approximations, although its derivation is based on very rough assumptions. Finally, Fig. 10 shows the dependence of the effective displacemant on the Mach number M_∞.

4.3.2 Questioning of Z_T

We are still confronted with the question whether the momentum transfer impedance Z_T (Equ. 1), which had been introduced to complete the acoustic boundary condition at sound absorbing walls with regard to the

[1] We regard the real-valued $k \in [-2, 2]$ as a free parameter here, irrespective of the parameters of the hypothetical sound propagation, e.g. the acoustic mode order, the boundary condition or the location of the sound source.

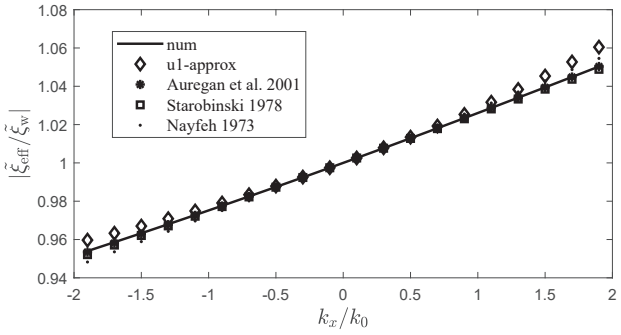

Figure 7. Effective displacement as a function of the normalized streamwise wavenumber k for $M_\infty = 0.1, 500$ Hz, and exponential mean flow.

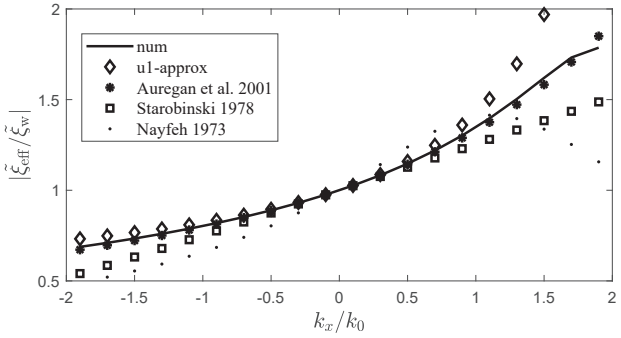

Figure 8. Effective displacement as a function of the normalized streamwise wavenumber k for $M_\infty = 0.4, 500$ Hz, and exponential mean flow.

momentum transfer between flow and wall [6, 7], is a local quantity independent of the structure of the sound field. $Z_\text{T}/(\rho_0\overline{u}_\infty)$ has been evaluated from the numerical solution of Eqn. 15 and 16, and $|Z_\text{T}/(\rho_0\overline{u}_\infty)|$ is shown in Fig. 11 as a function of $k_x c_0/\omega$ for various combinations of Mach number, frequency and flow profile. While the dependence on k_x is small at low Mach numbers, it cannot be disregarded at higher Mach numbers. Furthermore, with regard to perforated walls it had been earlier expected that $Z_T \propto \rho_0\overline{u}_\infty$ [7], which obviously does not apply to the homogeneous walls investigated here. However, in Fig. 11 it is obtained that $Z_T \propto \overline{u}_\infty^2$, so our concept of the momentum transfer by the wall shear stress was incomplete.

5 WALL WITH SEPARATED OPENINGS

Regarding the wall with macroscopic and separated openings ($L_\text{op}, L_\text{sp} \gg \delta_\nu, \delta_a$), the question arises how far the previous modeling of the unsteady flow over homogeneously permeable walls can be transferred to the inhomogeneous case. We will pursue this question in small steps:

5.1 Narrow unyielding slits and wide spacing

The mean flow remains homogeneous ($\mathrm{d}\bar{u}/\mathrm{d}x = 0$) because it is not affected by the narrow slits. The flow

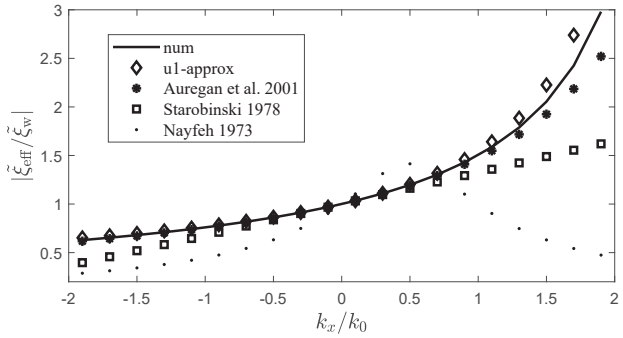

Figure 9. Effective displacement as a function of the normalized streamwise wavenumber k for $M_\infty = 0.4, 100$ Hz, and exponential mean flow.

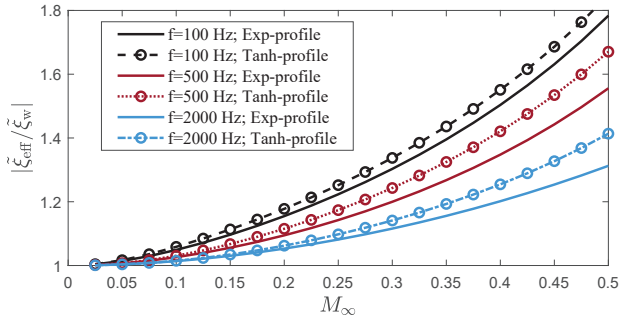

Figure 10. Effective displacement as a function of the Machnumber for different frequencies, mean flow profiles and $k = 1$ (numerical solution).

through the slits, which is caused by the superimposed sound, is impressed in this preliminary modelling according to the pressure distribution of a hypothetical sound wave ($\tilde{v}_{\text{op}} \sim \exp[i(\omega t - k_x x)]$) independent of the pressure that actually exists above the slits. The unsteady field

$$\tilde{\Phi}_m(x,y,t) = \tilde{v}_{\text{op}}^{(0)}(\omega)\, L_{\text{op}}\, e^{i(\omega t - k_x x)}\, \Phi^{(0)}(x - mL_{\text{sp}}, y, \omega) \tag{26}$$

which is excited at the m^{th} slit, then propagates unaffected by the other slits along the solid unyielding wall, and the total field is the linear superposition of all the individual fields

$$\begin{aligned}\tilde{\Phi}(x,y,t) =& \tilde{v}_{\text{op}}^{(0)}(\omega)\, L_{\text{op}}\, e^{i(\omega t - k_x x)} \ldots \\ & \ldots \sum_{m=-\infty}^{\infty} \Phi^{(0)}(x - mL_{\text{sp}}, y, \omega)\end{aligned} \tag{27}$$

which is a quasi periodic function of x that can be be represented as a sum of partial waves

$$\tilde{\Phi}(x,y,t) = \tilde{v}_{\text{w}}(\omega) \sum_{n=-\infty}^{\infty} \hat{\Phi}^{(0)}(n\kappa_{\text{sp}}, y, \omega) e^{i[\omega t + (nk_{\text{sp}} - k_x)x]} \tag{28}$$

with the Fourier transform $\hat{\Phi}^{(0)}(\kappa, y, \omega)$ with respect to x of $\Phi^{(0)}(x, y, \omega)$ and with $\kappa_{\text{sp}} = 2\pi/L_{\text{sp}}$; $\tilde{v}_{\text{w}} = \tilde{v}_{\text{op}}^{(0)} L_{\text{op}}/L_{\text{sp}}$ is the spatial average of the wall-normal velocity through

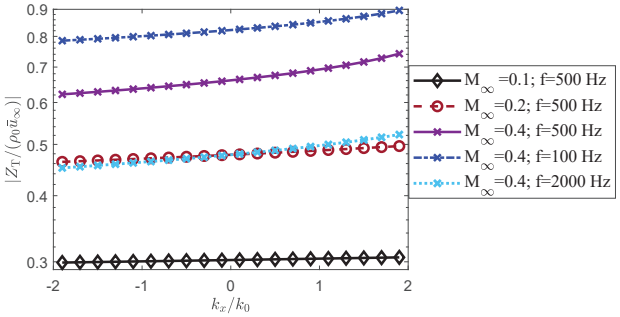

Figure 11. Magnitude of the normalized momentum transfer impedance Z_T as function of the streamwise wavenumber.

the wall. Each of the partial waves is connected with an added displacement, but only the displacement due to $n = 0$ exhibits a constant phase difference to the pressure of the hypothetical sound wave, and thus delivers a net contribution to the propagation of real sound waves. The amplitude of the partial wave mit $n = 0$, namely $\tilde{v}_{\text{w}} \int_{-\infty}^{\infty} \Phi^{(0)}(x, y, \omega) \mathrm{d}x$ is independent of the spacing L_{sp}, and thus is the same as for the homogeneous wall.

5.2 Narrow yielding slits and wide spacing

Next, we allow that the acoustic flow through the slits is controlled by the pressure above the slits: $\tilde{v}_{\text{op}} L_{\text{op}} = Y_{\text{op}} \tilde{p}(x_{\text{op}})$, where Y_{op} is the volume flow admittance of the opening. However, we neglect the pressure of the hydrodynamic and higher acoustic modes, i.e. we consider only the two fundamental modes propagating in a hard walled duct in $+x$- and $-x$-direction with wavenumbers $k^+ > 0$ and $k^- < 0$. The straightforward but lengthy calculation of the effective wavenumbers $k_{\text{eff}}^{\pm}$ that result due to the scattering at the slits, is based on the four-pole theory [2] and is skipped here. If we use $k^{\pm} = k_0/(M_{\text{avg}} \pm 1)$ with $k_0 = \omega/c$ and with Mach number M_{avg} that is averaged over the duct cross-section being a good approximation of the one-dimensional sound propagation in the hard-walled flow duct, we obtain with $k_0 L_{\text{sp}} \ll 1$

$$k_{\text{eff}}^{\pm} = \left[\pm \sqrt{1 - \frac{iY_{\text{w}}}{k_0 h (1 - M_{\text{avg}}^2)}} - M_{\text{avg}} \right] \frac{k_0}{1 - M_{\text{avg}}^2} \tag{29}$$

wherin h ist the height of the duct lined on one side, and $Y_{\text{w}} = Y_{\text{op}} L_{\text{sp}}$ is is the average acoustic admittance of the lining. It turns out that $k_{\text{eff}}^{\pm}$ is independent of L_{sp} and equals the well-known inviscid solution for the homogeneous flow duct with $k_0 h \ll 1$.

So far, only the scattering of the two fundamental sound modes has been considered, and the resulting independency from L_{sp} results from the fact that $k^{\pm} L_{\text{sp}} \ll 1$ can be assumed. This, however, does not necessarily apply

[2] The channel is sectioned into pieces of length L_{sp} and thus can be represented as a chain of equal four-poles; then the two eigenvalues of the chain matrix are the transmission factors $k_{\text{eff}}^{\pm} L_{\text{sp}}$ of the channel sections.

to the hydrodnamic modes. Thus, the mode conversion at the openings (see, e.g. [9, 10]) may provoke a dependency of the effective wavenumbers on the spacing of the openings though the pressure of the hydrodynamic modes is expected to be much smaller than the sound pressure.

5.3 Wide slits

Fig. 2 and 3 show sketches of the deflected streamlines above wide slits and of the mechanisms which might be caused by the sound induced displacement of this flow field. The question, whether, and if so, how these mechanisms contribute to the added displacement is completely open again, after a former assumption has turned out to be wrong, namely that the streamwise force, that acts on wall due to the stagnation pressure on the rear part of the opening, has the same effect on the added displacement as the wall shear stress.

6 CONCLUSION AND OUTLOOK

It has been shown that the acoustic wall shear stress and thus the momentum transfer impedance only indirectly describes the effect, which the momentum transfer between wall and flow has on the acoustic boundary condition of the wall. In addition the momentum transfer impedance depends on the sound wave number and is therefore not a local quantity.

Two types of liner surfaces are investigated, the homogeneously permeable wall and the wall with separate openings. Only the homogeneous wall has been considered in previous studies as a model for liner surfaces. The current investigation of homogeneous walls has been focussed on the propagation of the shear stress through the acoustic boundary layer and the exact solution has been compared to various approximations. Interestingly, the approximation by Aurégan et al. [3] performs very well, although its derivation is based on very rough assumptions.

The main purpose of the current project is to transfer the findings with homogeneous walls to inhomogeneous walls. For well separated narrow openings, which have no effect on the mean flow, the effective admittance is independent of the spacing and the size of the openings, if the mode conversion between acoustic and hydrodynamic modes at the openings is neglected. With wide openings the streamwise force on the wall is augmented by the stagnation pressure on the trailing edge of the opening. It has turned out, however, that the effect on the effective admittance strongly differs between the stagnation pressure and the wall shear stress.

ACKNOWLEDGEMENTS

The authors gratefully acknowledge the financial support of the German Research Foundation (project *SCHU 3376/2-1*). This work was produced during a research stay at Technical University Vienna in collaboration with Florian Toth and Manfred Kaltenbacher. The authors are grateful for the hospitality and the fruitful discussions.

7 REFERENCES

[1] A. H. Nayfeh, "Effect of the acoustic boundary layer on the wave propagation in ducts," *The Journal of the Acoustical Society of America*, vol. 54, no. 6, pp. 1737–1742, 1973.

[2] R. Starobinski, "Sound propagation in lining duct with essentially non-uniform distribution of velocity and temperature," in *Noise of jet engines, Issue 2, CIAM*, 752, pp. 155–181, 1978.

[3] Y. Aurégan, R. Starobinski, and V. Pagneux, "Influence of grazing flow and dissipation effects on the acoustic boundary conditions at a lined wall," *Journal of the Acoustical Society of America*, vol. 109, no. 1, pp. 59–64, 2001.

[4] E. J. Brambley, "Viscous boundary layer effects on the myers impedance boundary condition," in *15th AIAA/CEAS Aeroacoustics Conference, 11-13 May 2009, Miami, Florida*, 2009. AIAA-2009-3241.

[5] D. Khamis and E. J. Brambley, "Analytic model and concise impedance boundary condition for viscous acoustics in ducted shear flow," in *22th AIAA/CEAS Aeroacoustics Conference, 30 May-1 June 2016, Lyon, France*, no. AIAA 2016-2976, 2016.

[6] J. Rebel and D. Ronneberger, "The effect of shear stress on the propagation and scattering of sound in flow ducts," *Journal of Sound and Vibration*, vol. 158, pp. 469–496, 1992.

[7] A. Schulz, C. Weng, F. Bake, L. Enghardt, and D. Ronneberger, "Modeling of liner impedance with grazing shear flow using a new momentum transfer boundary condition," in *23rd AIAA/CEAS Aeroacoustics Conference, 5 - 9 June 2017, Denver, CO*, no. AIAA 2017-3377, 2017.

[8] Y. Aurégan, "On the use of a stress-impedance model to describe sound propagation in a lined duct with grazing flow," *The Journal of the Acoustical Society of America*, vol. 143, pp. 2975–2979, 2018.

[9] E. Meyer, F. Mechel, and G. Kurtze, "Experiments on the influence of flow on sound attenuation in absorbing ducts," *Journal of the Acoustical Society of America*, vol. 30, p. 165, 1958.

[10] F. Mechel, "Schalldämpfung und schallverstärkung in luftströmungen durch absorbierend ausgekleidete Kanäle," *Acustica*, vol. 10, no. 3, pp. 133–148, 1960.